Science Advances
AAAS

advances.sciencemag.org/cgi/content/full/5/4/eaav3482/DC1

Supplementary Materials for

Quantifying landslide frequency and sediment residence time in the Nepal Himalaya

D. M. Whipp* and T. A. Ehlers

*Corresponding author. Email: david.whipp@helsinki.fi

Published 24 April 2019, *Sci. Adv.* **5**, eaav3482 (2019)
DOI: 10.1126/sciadv.aav3482

This PDF file includes:

Supplementary Materials

Catchment bedrock age prediction

Bedrock thermochronometer ages are predicted in a 3D numerical model of the Marsyandi River region in central Nepal using a modified version of the software Pecube (*15, 16*) from which a subsample of ages is extracted from the Nyadi catchment to generate the catchment predicted age distribution (Fig. 2 in main text). The Pecube numerical model design is intended to simulate the first-order fault kinematics and heat transfer in the Himalaya of central Nepal (Fig. 2a in main text). The kinematic model has a single active fault, the model equivalent of the Main Himalayan thrust (MHT) that underlies the Himalaya with a fixed convergence velocity of 20 mm/a between stable India and Tibet (*34*) and slip partitioned between overthrusting and underthrusting. In the models we present, overthrusting fault motion results in a constant rock uplift rate of ~2.5 mm/a across the Nyadi catchment. Surface denudation in the model exactly balances rock uplift maintaining steady-state modern topography and exhuming rocks from depth to the surface of the model over a simulation time of 50 Ma. The thermal history recorded on tracking particles during exhumation is used to predict muscovite $^{40}Ar/^{39}Ar$ bedrock ages across the entire model surface. Predicted ages within a given catchment (Fig. 2b,c in main text) are then extracted from the full age population to form the catchment age population.

A probability distribution of ages in the catchment is created using a Gaussian distribution of uncertainty for each catchment age, summing the individual age probability distributions, and normalizing the area beneath the resulting curve to one (Fig. 2c in main text). To account for spatial variations in model exhumation rates in the catchment, the probabilities of occurrence of the ages in the catchment age population are scaled in proportion to the instantaneous exhumation rates at the surface in Pecube. Thus, the equation for the predicted probability density function (PDF_p) of age t for an individual predicted age t_p with standard deviation σ_{t_p} (*15, 17*) is

$$\mathrm{PDF}_p = \frac{1}{\sigma_{t_p}\sqrt{2\pi}} \exp\left(-\frac{1}{2}\left(\frac{t - t_p}{\sigma_{t_p}} \right)^2 \right) \times v_z$$

where v_z is the instantaneous exhumation rate at the location of the predicted age on the surface of the Pecube model. For the results in this paper, σ_{t_p} is calculated by multiplying the a given predicted age by the median percent uncertainty in the observed ages from the Nyadi catchment sample collected in 2002 (10.9%; (*17*)). For a set of n predicted ages extracted from the catchment age population, the predicted synoptic probability distribution function ($SPDF_p$) of age t is simply the sum of the individual PDF_p distributions normalized to the average instantaneous exhumation rate for the catchment $\bar{v}_z$, or

$$\mathrm{SPDF}_p = \frac{1}{n}\sum_{i=1}^{n} \mathrm{PDF}_p(i) \times \frac{1}{\bar{v}_z}$$

As noted above, the instantaneous exhumation rates in the Pecube model are constant across the Nyadi catchment. More information about the thermokinematic model design can be found in Whipp, Ehlers, Braun and Spath (*15*).

Landslide age prediction

Calculation of landslide-produced detrital age distributions involves sampling of the catchment ages by randomly placed landslides with a power-law frequency-area distribution, storage of the landslide-sourced ages over a given time interval (residence time), and random sampling of the resulting age population and calculation of the resulting age distributions. Within the catchment of interest (e.g., Fig. 2b in main text), landslides are positioned at random (e.g., fig. S1a) with their frequency and area determined by the power-law frequency-area relationship of Hovius, Stark and Allen (*13*) scaled to erode the catchment at the average exhumation rate across the catchment in the Pecube model following the method of Niemi, Oskin, Burbank, Heimsath and Gabet (*30*). Potential landslides that extend beyond the catchment area are randomly repositioned until their location is entirely within the catchment. The upper bound for the area of the landslides limits them to circles with a diameter of no more than 7 km, roughly the distance between ridges and valleys in the larger Marsyandi River to which the Nyadi is a tributary. However, the largest landslide expected even with a 10,000-year recurrence time would have a diameter of <4 km according to the power-law relationship, comparable to the average valley-ridge distance in the Nyadi catchment. Landslide-sampled ages and corresponding erosion rates are stored for a specified time interval, or residence time, by assuming a hemispheroidal geometry with a landslide depth equal to 5% of the slide width to produce the landslide age population.

Using the same method as described for creating the $SPDF_p$ for the whole catchment, ages are randomly selected from the landslide age population and used to create the landslide $SPDF_p$ for comparison with the observed age distribution(s). After creating the landslide $SPDF_p$ from a random sample of *n* ages in the landslide age populations, it is converted to a cumulative distribution by integrating across its age range. The cumulative $SPDF_p$ is then compared to the observed age distribution(s) for the Nyadi catchment (*17, 18*) using the two-sample Kuiper's test (*33*) with a significance level of $\alpha = 0.05$. The result of the test, whether or not the two age distributions are statistically similar or different, is then stored. The process of random age selection from the landslide age population, construction of the landslide $SPDF_p$ and comparison of the landslide $SPDF_p$ to the observed ages is repeated 10,000 times, ultimately providing a percentage of random samples of *n* ages that yield age distributions statistically indistinguishable from the observed age distributions (percent similar). An example of 100 $SPDF_p$ distributions for a residence time of 1 year is shown in fig. S1b, in which 8.2% of the landslide age distributions are statistically the same as the observed age distribution.

Lastly, based on the landslide frequency-area relationship of Hovius, Stark and Allen (*13*) it is possible to predict the recurrence interval for landslides of given sizes as a function of the catchment area (fig. S1c). The point here is that even the smallest landslides considered in this work ($A = 0.005$ km^2) are only predicted to occur infrequently in small catchments, which has important implications for the residence time of sediment produced by landslides in the catchment. For a catchment area of $A = 25$ km^2 the smallest landslides will only be recorded for residence times of 5 years or more, and the residence time must by 50 years or more to record the smallest landslides for a catchment area of $A = 5$ km^2. On this basis, we might reasonably expect small catchments to be quite sensitive to individual landslides and their resulting bias in the fraction of catchment bedrock ages they sample.

Landsliding in the Nyadi catchment

Our interpretation that poor reproducibility in detrital thermochronometer age distributions is the result of stochastic erosion requires demonstration that stochastic erosional processes such as landsliding occur within the basin from which samples were taken. To demonstrate the occurrence of landslides in the Nyadi catchment we have processed a set of Landsat 4-5 Thematic Mapper

images (fig. S2) to allow visual identification of individual landslides over the time period preceding and following sample collection in 1997 and 2002 catchment (*17, 18*). The images cover the years 1988-2011 and have been produced by combining bands 7 (Shortwave Infrared 2), 4 (Near Infrared), and 2 (visible green) as the red, green, and blue colors, respectively. With this band combination green image colors correspond to vegetated regions, red-orange colors indicate bedrock exposure, and snow cover is cyan. The contrast between colors allows for easy identification of landslides, particularly in vegetated regions. In some areas lacking vegetation or where the steep topography results in shadow effects (dark gray regions in fig. S2) we have not attempted to identify landslides. Regardless, comparison of the images for the time period of 1988-2011 shows clear evidence that landsliding is a common erosional process in the Nyadi catchment (fig. S2), and one that would be expected to affect the ages in collected sediment samples. Although it is possible to utilize the Landsat imagery to further quantify rates of bedrock erosion by landsliding, such an analysis is beyond the scope of this work.

Supplementary figures

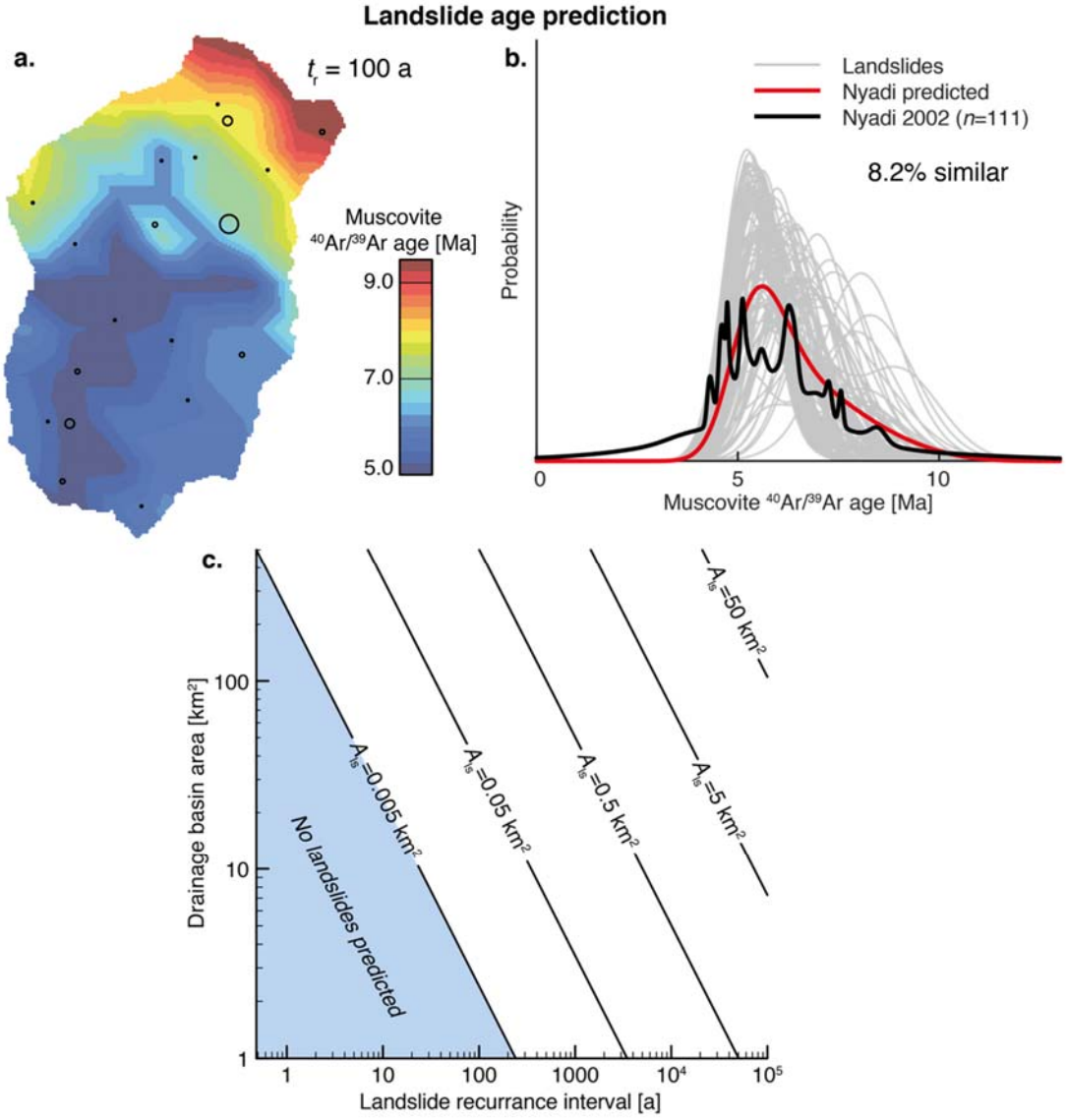

Fig. S1. Overview of landslide age prediction. (**a**) Example of random landslides (black circles) over a 100-year period in the Nyadi drainage basin with their frequency and area determined using the power-law landslide frequency-magnitude relationship of Hovius, Stark and Allen (*13*) scaled to a basin average erosion rate of 2.5 mm/a following the approach of Niemi, Oskin, Burbank, Heimsath and Gabet (*30*). In this example, there is one 0.24 km^2 landslide, two 0.12 km^2 landslides, five 0.06 km^2 landslides, and 11 0.03 km^2 landslides, which all sample different age populations in the catchment. (**b**) Example synoptic probability distribution functions for 100 random landslide-sampled age distributions with a sediment residence time of one year (gray lines) with the distribution of bedrock ages across the catchment (heavy red line). In this case 8.2% of the landslide age distributions are statistically equal to the catchment bedrock age distribution. (**c**) Recurrence time of landslides of different size as a function of the drainage basin area based on the power-law landslide frequency-magnitude relationship used in (a). The light blue region shades the basin area and recurrence interval combinations where no landslides would occur.

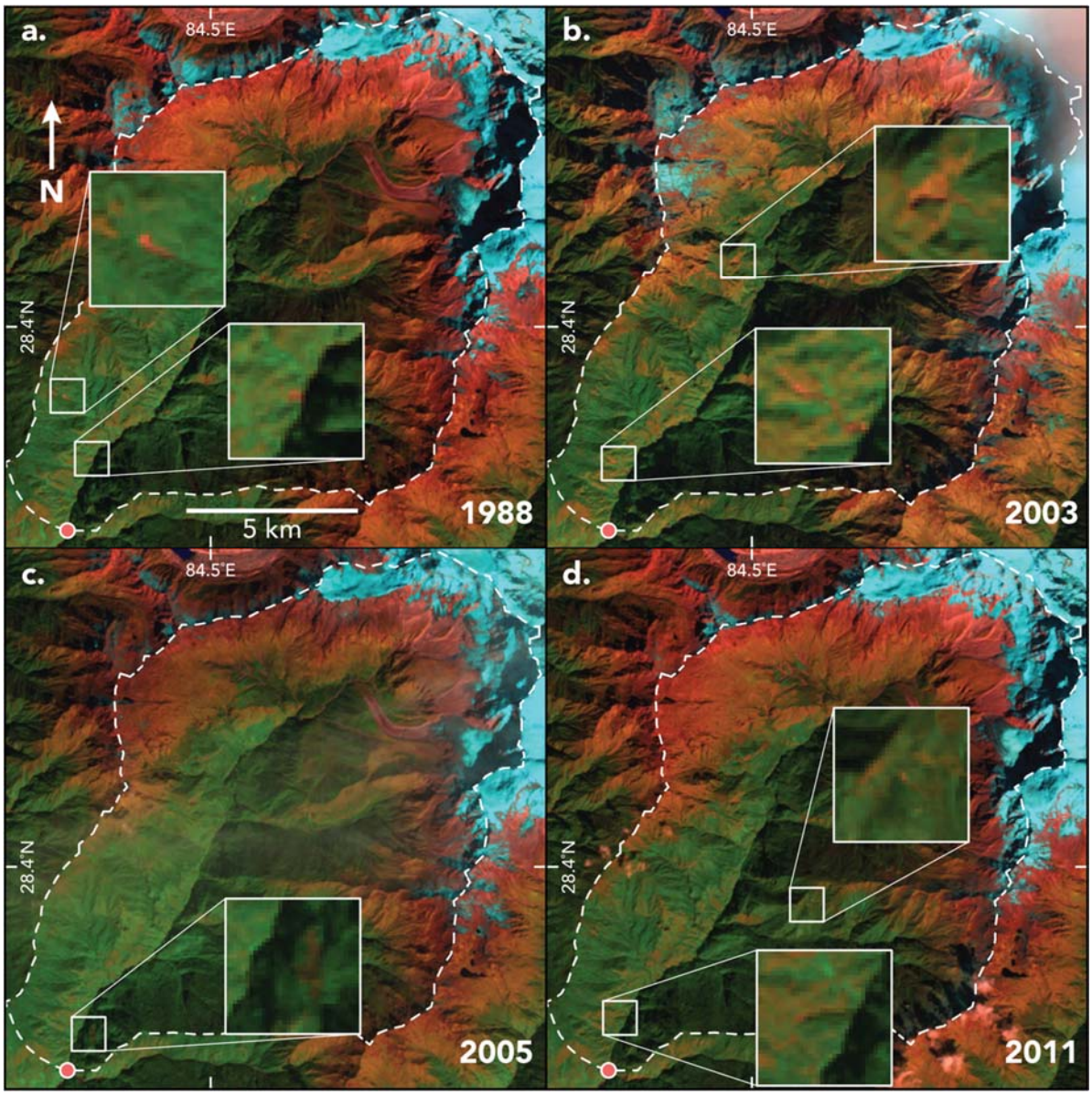

Fig. S2. Satellite imagery of landslides in the Nyadi catchment. False-color Landsat 4-5 Thematic Mapper imagery (bands 7, 4, and 2) of the Nyadi catchment over the period preceding and following collection of detrital thermochronometer samples in 1997 and 2002 that are used in this work (*17, 18*). Images from (**a**) October 19, 1988, (**b**) November 14, 2003, (**c**) October 18, 2005, and (**d**) October 19, 2011 show vegetated regions in green, exposed bedrock in red-orange, and snow cover in cyan. Landslides (inset zoomed boxes) are clearly visible as orange regions within in vegetated regions and their locations vary in the images providing an estimate of the frequency of landsliding in the Nyadi catchment. Landsat 4-5 Thematic Mapper imagery courtesy of the U.S. Geological Survey.